EEET ECOLOGICAL ENGINEERING & ENVIRONMENTAL TECHNOLOGY

Ecological Engineering & Environmental Technology 2024, 25(6), 20–26
https://doi.org/10.12912/27197050/186546
ISSN 2719-7050, License CC-BY 4.0

Received: 2024.03.21
Accepted: 2024.04.22
Published: 2024.05.01

Adsorption Isotherms and Kinetics Studies of Lead on Polyacrylonitrile-Based Activated Carbon Nonwoven Nanofibres

Basma I. Waisi[1*], Israa S. Al-Bayati[1], Asrar A. Alobaidy[1], Manal A. Mohammed[1]

[1] Department of Chemical Engineering, College of Engineering, University of Baghdad, Baghdad, Iraq

* Corresponding author's e-mail: basmawaisi@coeng.uobaghdad.edu.iq

ABSTRACT

Activated carbon nonwoven nanofibres (ACNN) mat derived from polyacrylonitrile was manufactured through the electrospinning method followed by thermal treatment steps. The ACNN ability to adsorb Pb(II) from a liquid solution was evaluated. The fabricated ACNN was characterized using scanning electron microscope, Fourier-transform infrared spectroscopy, and Brunauer-Emmett-Teller method. The resulting ACNN exhibited nanofibres with a diameter of 530 nm and a surface area of 550 m^2/g. Various adsorption experiments were performed in batch scale to study the impact of factors like contact time, initial Pb(II) ions concentration, and pH. At pH 5, ACNN achieved a removal efficiency of 98% of Pb(II). The equilibrium data for Pb(II) ions was analysed using the Freundlich and Langmuir isotherm models. Both kinetic models (pseudo-first-order and pseudo-second-order) and isotherm models were tested. Results revealed that the Langmuir model accurately described the adsorption isotherm of Pb(II) with a maximum capacity of 15.72 mg/g. Data analysis suggested that the pseudo-second-order model better represented the kinetic adsorption behaviour of Pb(II).

Keywords: activated carbon, adsorption, Pb(II), nanofibres.

INTRODUCTION

Inorganic heavy metal species and related metalloids are among the most problematic contaminants in surface water due to their challenging removal processes, complicated existence, minuscule concentration in large volumes, and competition with nontoxic inorganic species (Al-Bayati et al., 2023; Mohammed et al., 2023; Waisi et al., 2015). Pb(II) is recognised as a longstanding environmental contaminant. It exists in various industries effluents, including acid battery manufacturing, ceramic and glass factories, printing, tanning, photographic materials, metal planting and finishing (Momčilović et al., 2011). Pb(II) is a common metal with a harmful impact on the environment and the danger of water pollution for humans. Extended periods of Pb(II) exposure may result in infertility and miscarriage, in addition to causing damage to the health and nervous system of human (Dave and Chopda, 2014). Such a toxic material was needed to be extracted from the drainage system. A trace concentration of Pb(II) ions is also extremely hazardous (Wani et al., 2015). The permissible Pb(II) concentration in potable water, as mandated by the Environmental Protection Agency (EPA) of the United States, is 0.015 mg/L. The most common treatment technologies for metal ions elimination are precipitation (Onundi et al., 2011), phytoremediation (Saxena et al., 2020), electrocoagulation (Shakir and Husein, 2009), and ion exchange (Chanthapon et al., 2018). Membrane technology is considered an efficient method to treat polluted water, but its disadvantages are high energy consumption and fouling. In addition, the adsorption treatment method is widely used for heavy metal removal because of its consistency and simplicity (Kalash et al., 2020). To adsorb a trace amount of pollutants, especially heavy metals, the adsorbent material, such as activated carbon, should

have a large surface area, unique microstructure, high adsorption capacity, and good selectivity. Nano-form adsorbent materials such as nanoparticles, nanotubes, and nanofibres are widely applied in extracting the dissolved heavy metal ions (Dave and Chopda, 2014). Activated carbon nonwoven nanofibres (ACNN) are nanofibre form adsorbents. They are fabricated by electrospinning method followed by thermal treating steps. In the electrospinning technique, the precursor nanofibres are created from polymeric solution in a voltage field to overcome the surface tension of the polymeric droplet. Commonly, the polyacrylonitrile (PAN) polymer is used in preparing ACNN, because of its yield and thermal characteristics (Waisi, 2019). The thermal treatment stage consists of carbonisation under the N_2 atmosphere at a temperature of 800 °C to convert the precursor fibres to carbon fibres. Then, the activation stage can be physically (using steam) or chemically (using chemicals such as H_2SO_4 and HNO_3) processed at high temperatures (Fan et al., 2011). The ACNN generated displays features like having a surface area that is easy to access pores of moderate size and fibres on a nanoscale (Waisi et al., 2023). This specific carbon material has been utilised in energy storage, cleaning air and treating water (Alkarbouly and Waisi, 2022; Waisi et al., 2020). The ACNN mats have been applied to remove contaminants like cations, toluene, formaldehyde and emulsified oil (Oh et al., 2008; Waisi et al., 2020, 2023). However, little attention has been focused on using the ACNN material for adsorption of heavy metals. The adsorption capacity of heavy metals is mainly affected by the porous structure and the surface chemistry of the adsorbent material. Using the electrospinning technique can help in producing aligned nanofibres. Then, controlling the carbonization and Activation stages can provide the nanofibre material with the necessary functional groups that increase the interaction between heavy metal ions and ACNN fibres. In this work, the electrospinning method fabricated the PAN-based ACNN sheet. Then, the surface morphology, pores construction, and surface chemistry of the fabricated ACNN sheets were explored by SEM, BET, and FTIR analysis. Then, it was applied in Pb(II) removal from water using batch mode tests to understand the isotherm and kinetics of the process by investigating the effect of the initial solution pH and ACNN sheets dose over time.

MATERIALS

Polyacrylonitrile (Mwt. = 150,000 g/mol) was ordered from Scientific Polymer Products Inc. N,N-dimethylformamide (DMF) was obtained from Sigma Aldrich (USA). Sodium hydroxide (NaOH) and hydrochloric acid (HCl) were acquired from Sigma Aldrich, United States of America. Analytical grade of $Pb(NO_3)_2$ (purity = 99% and Mwt. = 331.2 g/mol from Sigma Aldrich, USA) was used to prepare 1000 mg/L standard stock solution of Lead (II).

Preparation of the adsorbent

A certain amount of the polymer is mixed with the DMF solvent under a continuous mixing for 2 h at 60 °C to prepare 12 wt.% PAN/DMF. The precursor solution was dispensed using an electrospinning system fitted with a revolving 70 rpm grounded collector tank. A high pressure syringe pump (KD Scientific) fitted as an electrospinning nozzle with a needle of 20 gauges to deliver the polymer solution to the collector drum. The voltage applied was 21 kV with a fixed distance from the collector (18 cm). The fabricated precursor nanofibre mats were then stabilised in the air in a muffle furnace (Carbolite) at 280 °C for 1 h with 1°C/min ramp rate. After carbonisation and activation, the stabilised nanofibres were transformed into activated carbon nonwoven nanofibres. The carbonisation step was carried out in a furnace (Thermo Scientific Lindberg Blue M Tube Furnace) in an N_2 gas at 650 °C within 1 h with a 3 °C/min ramp rate. Then, the activation process was carried out in the same furnace with steam (60 g/h) at 750 °C for 1 h to produce the activated carbon nonwoven nanofibres. Authors' previous research describes the optimal conditions in detail (Waisi et al., 2019).

The characterizations

The scanning electron microscopy technique was used to examine the surface structure of ACNN using (FESEM, JEOL 6335F). The functional groups accountable for the binding of lead ions were identified using an Fourier-transform infrared spectroscopy (FTIR) within the 4000–500 cm^{-1} region. Micromeritics instrument

corporation analyzer was used for determining N_2 adsorption/desorption isotherms on the adsorbent material. The precise surface area of every sample was determined by utilising the Brunauer-Emmett-Teller (BET) model. The supernatant liquid was analysed at different time intervals using ICP-MS after separating the ACNN with nitrocellulose filter paper to make it adsorbent-free. The dissolved Pb(II) samples were acidified to 2% HNO_3 (trace metal grade) and examined using a plasma-mass spectrometer that is inductively linked (Agilent 7700x with Helium collision cell, ICP-MS).

Batch adsorption experiments

The simulated lead ions solution was prepared by diluting the prepared standard stock solution of Pb(II) with distilled water. Batch experiments were carried out by contacting 200 mg ACNN with 250 ml of Pb(II) solution in a plastic flask to determine the adsorption isotherms of Pb(II) on ACNN. The experiments were performed using a magnetic stirrer (400 rpm) at room temperature for 5 h. The impact of adsorption factors on the rate of the removal process were observed by varying ACNN dose (25, 50, and 200 mg) and initial solution pH (3, 4, 5, and 6) over time. The retained Pb ions concentration in the adsorbent phase (q) and the removal percentage (R%) were calculated according to Equations 1 and 2, respectively.

$$q = (C_i - C_t)\, V/W \tag{1}$$

$$R\,(\%) = (C_i - C_t) \times 100/C_i \tag{2}$$

The C_i is the initial Pb(II) concentration (mg/L); Ct is the Pb(II) concentration in the solution during the experiment (mg/L); V is the aqueous solution volume (L); and W is the weight (g) of ACNN. All experiments were duplicated, and the average result was depended for the further calculation. The flasks were sealed and stopped off to prevent pH fluctuations caused by gas exchange throughout the experiment.

RESULTS AND DISCUSSION

The characterization of ACNN

Figure 1 displays the surface morphology and cross-sectional scanning electron micrographs of ACNN sheets based on 12% PAN/DMF. Figure 1a shows the surface morphology of the ACNN sheet, which consists of long, continuous, and beads-free nanofibers in a nonwoven structure. The average fibre size was about 530 nm, with a homogeneous size distribution. According to the ACNN sheets, cross-sectional morphology

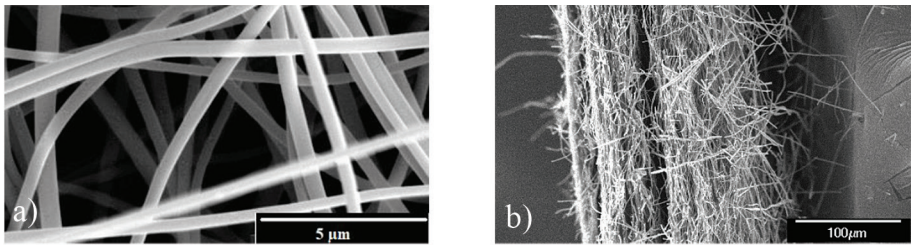

Figure 1. The images in SEM of the prepared ACNN sheets: (a) surface and (b) cross-section morphologies

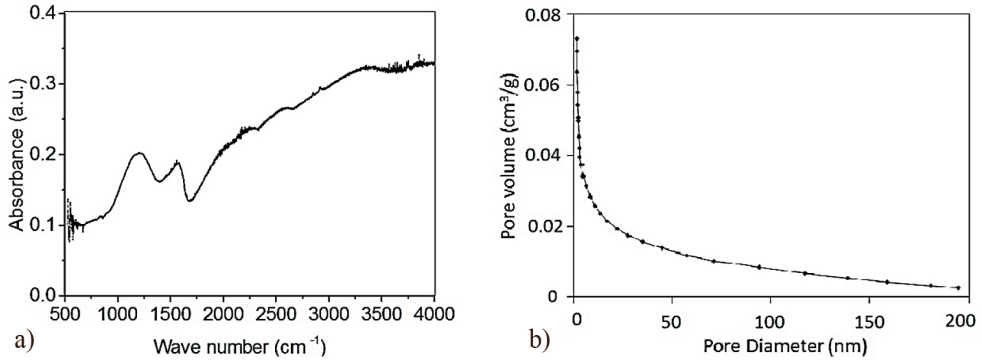

Figure 2. The ACNN analysis (a) FTIR spectrum and (b) pore size measurement from BET analysis

(Figure 1b) has a nonwoven structure with a thickness of approximately 160 µm.

The FTIR surface chemistry of ACNN sheets is illustrated in Figure 2a. The primary peak group seen at 1160 cm^{-1} is associated with the phenolic group's O-H bond produced by the steam activation step. The intensity of the peak at 1580 cm^{-1} increases along with carbonyl groups during the activation by steam (Karra et al., 2013). Denitrogenation reactions occur in the activation stage, facilitating the elimination of structural imperfections and non-carbon components (including sulphur, oxygen, and nitrogen) while also contributing to forming sheet-like structures.

Furthermore, typical N_2 adsorption/desorption isotherm for ACNN is illustrated in Figure 2b. Under the IUPAC classification, this is called type II adsorption. According to the adsorption isotherm of ACNN, most pores were microporous and mesoporous, measuring less than 50 nm in diameter.

Impact of the adsorption parameters

Impact of pH solution

While holding all other parameters constant (5% initial ion concentration and 0.2 g ACNN dosage, Figure 3 illustrates the Pb(II) removal by ACNN mats at various pH levels. At a pH of 5, the maximum degree of Pb(II) elimination was 98%. A clear improvement in the efficacy of Pb(II) adsorption was noted when the pH of the aqueous solution rose from 3 to the optimal value of 5. The fabricated ACNN absorb Pb(II) under acidic conditions with reduced efficiency, as seen by the subsequent dramatic decrease in value with decreasing pH. This may be deduced from the pH_{PZC} value, representing the zero charge point for activated carbon nanofibers. The pH_{PZC} ranges from 5 to 6 (Mahmood and Waisi, 2021). At pH values below pH_{PZC}, the surface of ACNN mats exhibits a positive charge, whereas it demonstrates a negative charge above that point. When the surface is positively charged, adsorption sites become encased in hydronium ions (H_3O^+). As a result, the repulsive interactions between metal ions and adsorbent surfaces diminish. Hence, an adsorption process is more effectively conducted at a pH greater than pH_{PZC}. Nevertheless, as the pH level approaches or exceeds six, the metal ions precipitate as salts, impeding the adsorption.

Impact of adsorbent dosage

According to Figure 4, the adsorption of Pb (II) ions increased as the adsorbent amount was raised from 25 mg to 200 mg because of increasing the availability of adsorbing sites at elevated doses. The maximum adsorption was recorded at the ACNN dose of 200 mg with 98% elimination of Pb(II) ions.

Impact of contact time

The influence of contact time on the uptake of Pb(II) ions on ACNN is illustrated in Figure 5. The obtained result showed a rapid increase in the Pb(II) ions uptake on ACNN material in the first 1 hr to reach 92% removal percentage due to the fast interactions between the effective sites of the (ACNN) adsorbent and the accumulation of

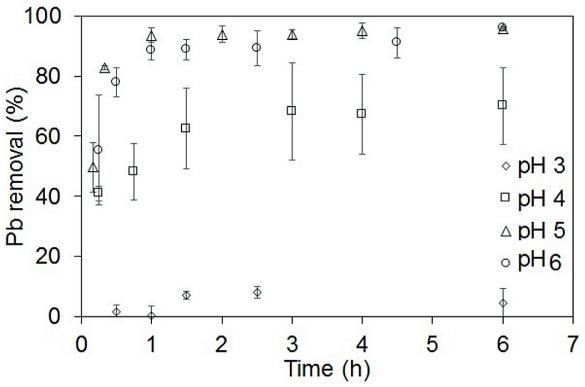

Figure 3. Impact of the solution pH on Pb(II) ions adsorption on ACNN. The experiment conditions were 25 °C, 400 rpm, 200 mg ACNN, and 5 mg/L initial Pb(II) concentration

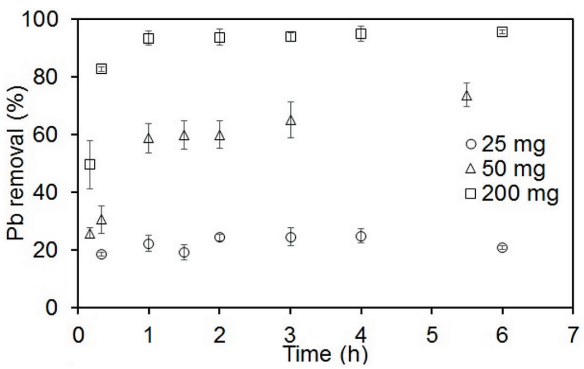

Figure 4. The impact of ACNN dose on the effectiveness of adsorption. The experiment conditions were 25 °C, 400 rpm, pH = 5, and 5 mg/L initial Pb(II) ions concentration

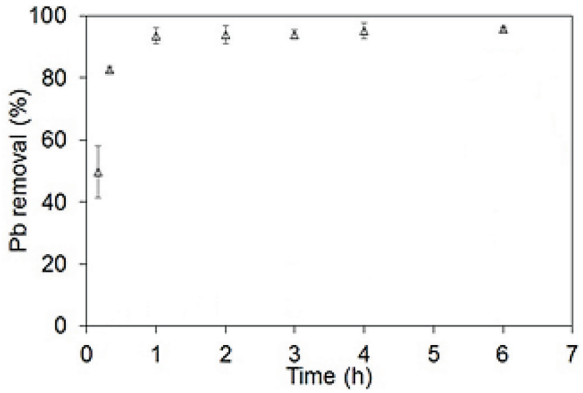

Figure 5. The effectiveness of ACNN in Pb(II) adsorption over time. The experiment conditions were 25 °C, 400 rpm, 200 mg ACNN, pH = 5 and 5 mg/L initial Pb(II) ions concentration

Pb(II) ions on the adsorbent surface. This can be explained by the fact that the high porous structure of ACNN offers a lot of binding sites on the adsorbent surface. The less plentiful supply of active causes the Pb(II) ions adsorption to become constant once it reaches equilibrium.

Adsorption isotherm

Langmuir and Freudlich isotherm models are represented by:

$$C_e/q_e = 1/K_L q_{max} + (1/q_{max}) \times C_e \quad (3)$$

$$Log\ q_e = Log\ K_F + (1/n) \times Log\ C_e \quad (4)$$

where: the equilibrium Pb(II) ions concentration is C_e (mg/L), the Pb(II) amount adsorbed at equilibrium is q_e, the maximum adsorption capacity is q_{max}, the power of the isotherm is n, and the equilibrium constants of Langmuir and Freundlich models are K_L and K_F, respectively. Figure 6 shows that Pb ions adsorption data fitted Langmuir model more than Freundlich model.

Kinetic modelling

The pseud-first and pseudo-second order kinetic models were applied to examine Pb(II) adsorption kinetic characteristics onto ACNN. These models can be represented in linear form as follows:

$$log\ (q_e - q) = log\ q_e - (k_1/2.303) \times t \quad (5)$$

$$t/q = 1/k_2 q_e^2 + (1/q_e) \times t \quad (6)$$

where: q_e and q, in mg/g, represent the Pb(II) adsorption uptake at equilibrium and at time (t), respectively, and K_1 and K_2 is the constants of adsorption rate in the first and second order kinetic models, respectively. The adsorption rate constants (K_1 and K_2) and the quantity of adsorption in equilibrium (q_e) are predicted using the slope and intercept of the linear plot (Figure 7), with the findings presented in Table 2.

Table 1. The coefficients of Langmuir and Freundlich models for the adsorption of Pb(II) on ACNN

Adsorption isotherm model	Parameter	Value
Langmuir	q_{max} (mg/g)	15.72
	K_L	8.26
	R^2	0.992
Freundlich	K_F (mg/g)	2.96
	n	3.19
	R^2	0.762

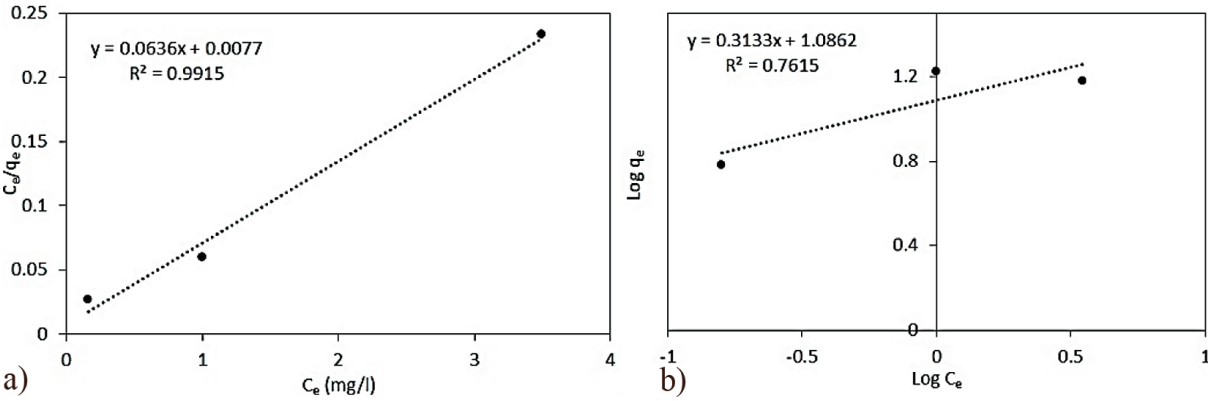

Figure 6. The Pb(II) adsorption isotherm models on ACNN (a) Langmuir (b) Freundlich. The experiment conditions were 25 °C, 400 rpm, 200 mg ACNN, 5 mg/L initial Pb(II) ions concentration, and 5 h contact time

Table 2. Rate constants for lead adsorption on ACNN

Adsorption kinetic model	Parameter	Value
Pseudo-first-order	q_e, mg/g	1.5077
	K_1, 1/min	1.76
	R^2	0.764
Pseudo-second-order	q_e, mg/g	6.04
	K_2 g/mg. min	2.58
	R^2	0.9995

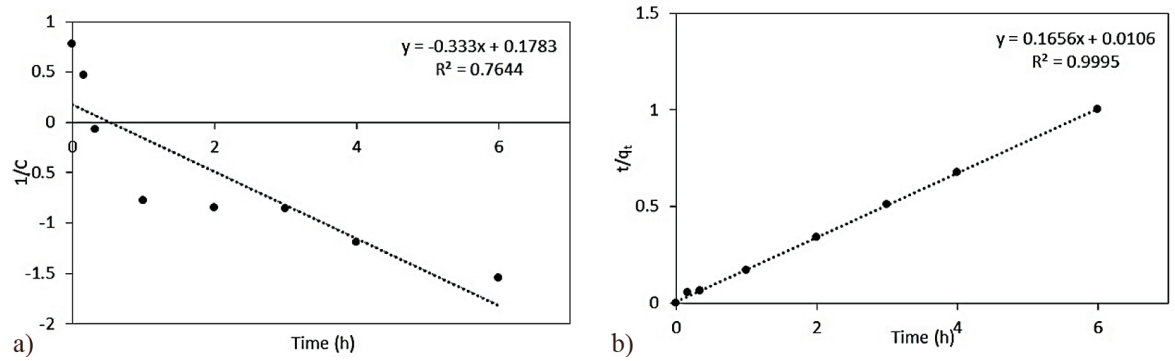

Figure 7. Adsorption kinetic models for Pb adsorption on ACNN (a) pseudo-first and (b) pseudo-second order

CONCLUSIONS

This work included preparing the activated carbon nonwoven nanofibres via the electrospinning method using polymeric precursor solution (PAN/DMF) and thermal treatment. The prepared ACNN was applied to remove Pb(II) ions from water. This research aimed to examine the effects of pH, adsorbent dose, and contact duration using batch sorption. Because no more sites were available for the adsorbent to capture Pb(II) ions, the adsorption was at its quickest after 30 minutes and remained almost constant after one hour. Lead removal efficiency of 98% was achieved at pH 5 with respect to lead ion removal. Furthermore, the results show that the prepared ACNN had excellent adsorption efficiency of Pb(II) due to its unique characteristics, such as the porous structure, the accessible high surface area, and the effective chemical functional groups on the surface.

REFERENCES

1. Al-Bayati, I.S., Abd Muslim Mohammed, S., Al-Anssari, S., 2023. Recovery of methyl orange from aqueous solutions by bulk liquid membrane process facilitated with anionic carrier, in: AIP conference proceedings. American Institute of Physics Inc. Feb 13, 2414(1). https://doi.org/10.1063/5.0114631
2. Alkarbouly, S.M., Waisi, B.I., 2022. Fabrication of electrospun nanofibers membrane for emulsified oil removal from oily wastewater. Baghdad Sci. J. 19, 1238–1248. https://dx.doi.org/10.21123/bsj.2022.6421
3. Chanthapon, N., Sarkar, S., Kidkhunthod, P., Padungthon, S., 2018. Lead removal by a reusable gel cation exchange resin containing nano-scale zero valent iron. Chem. Eng. J. 331, 545–555. https://doi.org/10.1016/j.cej.2017.08.133
4. Dave, P.N., Chopda, L.V., 2014. Application of iron oxide nanomaterials for the removal of heavy metals. J. Nanotechnol. 1–14. https://doi.org/10.1155/2014/398569
5. Fan, Z., Yan, J., Wei, T., Zhi, L., Ning, G., Li, T., Wei, F., 2011. asymmetric supercapacitors based on Graphene/MnO2 and activated carbon nanofiber electrodes with high power and energy density. Adv. Funct. Mater. 21, 2366–2375. https://doi.org/10.1002/adfm.201100058
6. Kalash, K.R., Alalwan, H.A., Al-furaiji, M.H., Alminshid, A.H., Waisi, B.I., 2020. Isothermal and kinetic studies of the adsorption removal of Pb (II), Cu (II), and Ni (II) Ions from Aqueous Solutions using Modified Chara Sp. Algae. Korean Chem. Eng. Res. 58, 301–306. https://doi.org/10.9713/kcer.2020.58.2.301
7. Karra, U., Manickam, S.S., McCutcheon, J.R., Patel, N., Li, B., 2013. Power generation and organics

removal from wastewater using activated carbon nanofiber (ACNF) microbial fuel cells (MFCs). Int. J. Hydrogen Energy, 38, 1588–1597.

8. Mahmood A., O., Waisi, B.I., 2021. Synthesis and characterization of polyacrylonitrile based precursor beads for the removal of the dye malachite green from its aqueous solutions. Desalin. Water Treat. 216, 445–455. https://doi.org/10.5004/dwt.2021.26906
9. Mohammed, M.A., Al-Bayati, I.S., Alobaidy, A.A., Waisi, B.I., Majeed, N., 2023. Investigation the efficiency of emulsion liquid membrane process for malachite green dye separation from water. Desalin. Water Treat. 307, 190–195. https://doi.org/10.5004/dwt.2023.29903
10. Momčilović, M., Purenović, M., Bojić, A., Zarubica, A., Ranđelović, M., 2011. Removal of lead (II) ions from aqueous solutions by adsorption onto pine cone activated carbon. Desalination, 276, 53–59. https://doi.org/10.1016/j.desal.2011.03.013
11. Oh, G., Ju, Y., Kim, M., Jung, H., Kim, H. jin, lee, W.-J., 2008. Adsorption of toluene on carbon nanofibers prepared by electrospinning. Sci. Total Environ. 393, 341–347. https://doi.org/10.1016/j.scitotenv.2008.01.005
12. Onundi, Y.B., Mamun, A.A., Khatib, M.F. Al, Saadi, M.A. Al, Suleyman, A.M., 2011. Heavy metals removal from synthetic wastewater by a novel nanosize composite adsorbent, 8, 799–806.
13. Saxena, G., Purchase, D., Mulla, S.I., Saratale, G.D., Bharagava, R.N., 2020. Phytoremediation of heavy metal-contaminated sites: Eco-environmental concerns, field studies, sustainability issues, and future prospects. Rev. Environ. Contam. Toxicol. 249, 71–131. https://doi.org/10.1007/398_2019_24
14. Shakir, I.K., Husein, B.I., 2009. LEAD Removal from Industrial Wastewater by Electrocoagulation process. Iraqi J. Chem. Pet. Eng. 10, 35–42. https://doi.org/10.31699/IJCPE.2009.2.4
15. Waisi, B., Arena, J.T., Benes, N.E., Nijmeijer, A., McCutcheon, J.R., 2020. Activated carbon nanofiber nonwoven for removal of emulsified oil from water. Microporous Mesoporous Mater. 296, 109966. https://doi.org/10.1016/j.micromeso.2019.109966
16. Waisi, B.I., 2019. Carbonized copolymers nonwoven nanofibers composite : surface morphology and fibers orientation. Iraqi J. Chem. Pet. Eng. 20, 11–15. https://doi.org/10.31699/IJCPE.2019.2.2
17. Waisi, B.I., Al-Furaiji, M.H., McCutcheon, J.R., 2023. Activated carbon nanofibers nonwoven flat sheet for methylene blue dye adsorption: batch and flow-through systems. Desalin. Water Treat. 289, 228–237. https://doi.org/10.5004/dwt.2023.29449
18. Waisi, B.I., Al-jubouri, S.M., McCutcheon, J.R., 2019. Fabrication and characterizations of silica nanoparticle embedded carbon nanofibers. Ind. Eng. Chem. Res. 58, 4462–4467. https://doi.org/10.1021/acs.iecr.8b05825
19. Waisi, B.I.H., Karim, U.F. a., Augustijn, D.C.M., Al-Furaiji, M.H.O., Hulscher, S.J.M.H., 2015. A study on the quantities and potential use of produced water in southern Iraq. Water Sci. Technol. Water Supply 15, 370. https://doi.org/10.2166/ws.2014.122
20. Wani, A.L., Ara, A., Usmani, J.A., 2015. Lead toxicity: a review. Interdiscip. Toxicol. 8, 55–64. https://doi.org/10.1515/intox-2015-0009